# Investigation of glass-fibre-reinforced-polymer shells as formwork and reinforcement for concrete columns[1]

**Shamim A. Sheikh, S.A.D. Jaffry, and Ciyan Cui**

**Abstract:** An investigation was conducted to study the behaviour of full-scale concrete-filled glass-fibre-reinforced-polymer (GFRP) shells under concentric compression. The main objective was to assess the suitability of prefabricated GFRP shells for stay-in-place formwork and confining reinforcement for columns. Seventeen columns, 356 mm in diameter and 1524 mm long were tested. The nominal target concrete compressive strength at 28 d was 30 MPa. Variables examined included number of GFRP layers, fibre orientation, and amount of longitudinal and lateral steel. Confinement by GFRP shells resulted in concrete response that displayed increased strength and associated strain followed by a ductile descending branch. Fibres in the longitudinal direction improved the load-carrying capacity of the columns, but the increase was less than the capacity of the fibres determined from the tension tests. Glass-fibre-reinforced-polymer shells also eliminate the need for closely spaced confinement steel, which should improve the quality of construction. In addition to ease of construction, GFRP shells provide protection against environmental effects, thus helping to reduce life cycle costs.

*Key words:* columns, confinement, stay-in-place formwork, strength, ductility, energy capacity, earthquake, seismic resistance, lateral reinforcement, glass-fibre-reinforced-polymer (GFRP) shell.

**Résumé :** Une étude a été réalisée à pleine échelle pour examiner le comportement d'enveloppes en polymère renforcé de fibres de verre (« GFRP ») remplies de béton sous compression concentrique. L'objectif principal était d'évaluer la possibilité d'utiliser des enveloppes « GFRP » préfabriquées comme coffrage permanent et renforcement de confinement de colonnes. Dix-sept colonnes de 356 mm de diamètre et de 1524 mm de longueur ont été mises à l'épreuve. La résistance nominale en compression cible du béton à 28 jours était de 30 MPa. Les variables examinées comprenaient le nombre de couches de « GFRP », l'orientation des fibres et la quantité d'acier longitudinal et latéral. Le confinement par des enveloppes « GFRP » a engendré une augmentation de la résistance et des déformations associées suivies d'une courbe descendante de la ductilité. Les fibres dans la direction longitudinale ont amélioré la capacité portante des colonnes mais l'augmentation était inférieure à la capacité des fibres déterminée lors des essais de traction. Les enveloppes « GFRP » ont également éliminé le besoin de barres d'acier de confinement rapprochées, ce qui devrait améliorer la qualité de construction. Les enveloppes « GFRP » fournissement également une protection contre les impacts de l'environnement en plus de faciliter la construction, aidant ainsi à réduire le coût du cycle de vie.

*Mots-clés :* colonnes, confinement, coffrage permanent, résistance, ductilité, capacité énergétique, séisme, résistance sismique, armature latérale, enveloppe en polymère renforcé de fibres de verre (« GFRP »).

[Traduit par la Rédaction]

## Introduction

Many observations have led to the conclusion that brittle column failures can result in total collapse of structures, particularly during severe earthquakes. For non-seismic design of columns, steel spirals with small pitch, similar to those required for seismic design, are used to take advantage of the improved column ductility and smaller capacity reduction for limit state design. Several researchers (e.g., Sheikh and Uzumeri 1980; Saatcioglu and Ozcebe 1989; Sheikh and Yeh 1990; Azizinamini et al. 1992) have reported that suitably arranged internal longitudinal and transverse steel reinforcement at close spacing is needed to produce ductile columns. The tightly knit cages produce difficult conditions for casting of concrete, resulting in low-quality construction. This study investigated the use of glass-fibre-reinforced-polymer (GFRP) shells for stay-in-place forms and for confining reinforcement for columns, in an attempt to eliminate the need for closely spaced steel reinforcement. The shells can also protect the encased concrete and steel against harsh environmental effects, including salt attack, thus reducing the life cycle cost of the structure without significantly in-

Received 25 November 2005. Revision accepted 24 July 2006. Published on the NRC Research Press Web site at cjce.nrc.ca on 2 May 2007.

**S.A. Sheikh,[2] S.A.D. Jaffry, and C. Cui.** Department of Civil Engineering, University of Toronto, 35 St. George Street, Toronto, ON M5S 1A4, Canada.

Written discussion of this article is welcomed and will be received by the Editor until 31 July 2007.

[1]This article is one of a selection of papers in this Special Issue on Intelligent Sensing for Innovative Structures (ISIS Canada).

[2]Corresponding author (e-mail: sheikh@ecf.utoronto.ca).

 doi:10.1139/L06-110 

creasing the initial capital cost. Work reported here is also applicable to columns retrofitted with wrapping and bonding of GFRP sheets or straps.

The idea of confining concrete columns using lateral steel was originally put forward by Considère (1903). Richart et al. (1928, 1929) carried out extensive research on spirally reinforced and hydraulically confined columns. More recent work (Table 1) on the confinement of concrete columns has involved the use of fibre-reinforced polymer (FRP) in place of steel. An extensive literature search revealed 672 tests on FRP-wrapped columns under concentric load, of which only 76 specimens had a diameter larger than 160 mm; and only 59, larger than 200 mm. To investigate the effect of lateral FRP reinforcement on the behaviour of columns, 636 specimens were selected in which either no lateral steel reinforcement was used or its spacing was greater than the diameter of the concrete core. Of these 636 tests (Table 1), only 52 specimens had diameters larger than 160 mm and only 35 specimens were larger than 200 mm in diameter, including 16 columns (356 mm in diameter) tested at the University of Toronto (Cairns and Sheikh 2001; Jaffry and Sheikh 2001). Only three columns with a diameter larger than 356 mm have been found in the literature (Kestner et al. 1997). Compared with the database on steel-confined columns, that on FRP-confined columns tested under concentric compression is obviously very limited, particularly on large specimens.

It can be seen from Table 1 that almost all the small-scale FRP-confined specimens had no post-peak response, whereas most of the large-scale columns displayed a stable descending branch of response under concentric compression. Data from large columns are thus needed for a full understanding of the complete behaviour of concrete confined with FRP that shows brittle elastic response under direct tension.

## Experimental setup

### Specimens

Seventeen large-scale circular concrete columns were designed, constructed, tested, and analysed (Jaffry and Sheikh 2001). All the specimens were 356 mm in diameter and 1524 mm long. Eleven of the 17 columns had glass FRP shells. The three main types of specimens were as follows: (*i*) specimens with neither longitudinal nor lateral steel; (*ii*) specimens with longitudinal steel and steel hoops at 320 mm spacing; and (*iii*) specimens with longitudinal steel and steel spirals at 75 mm pitch. Within each set, columns differed from each other in terms of the number of GFRP layers in the shells and the direction or orientation of the GFRP layers. Table 2 provides the details of the specimens.

The alphanumeric characters in the names of the specimens (Tables 2 and 3) provide information about their configuration. The letter “G” represents the presence of GFRP shell (omitted when there is no shell). The digit after the letter “G” represents the number of layers of glass fibres in the longitudinal direction; the second digit, layers in the lateral direction. If the fibres are oriented at 45°, this information is indicated before the number of fibre layers is given. The letter “L” after the numbers indicates the presence of longitudinal steel; “0” replaces “L” for specimens without longitudinal steel. The letter “S” indicates the presence of transverse steel, while “0” means that no transverse steel was provided. This is followed by the spacing (in millimetres) of the lateral steel. Finally, the last number indicates the specimen number. Hence, G01-LS320-10 means no glass fibre in the longitudinal direction, one layer of glass fibre in the lateral direction, and longitudinal reinforcement with lateral steel spaced at 320 mm; the specimen number is 10. Specimens 1 and 2 were plain concrete specimens without any GFRP shell. These specimens were reinforced with only one longitudinal bar in the centre for the purpose of handling the specimen safely before and after testing. In the designation of these two specimens, the number “1”, denoting only one longitudinal bar in the specimen, replaces the letter “L” for longitudinal steel.

### Concrete

Ready-mix concrete with a 28 d nominal compressive strength of 30 MPa was used for the construction of all the specimens. The concrete slump was 150 mm. Nineteen 150 mm × 300 mm concrete cylinders were cast with the columns and tested at various ages after casting. According to standard C39/C39M (ASTM 2000*b*), the 28-d concrete cylinder strength ranged between 29.0 and 30.3 MPa, with an average of 29.8 MPa. Longitudinal compressive strain at peak stress varied between 0.0018 and 0.0019.

### Steel

Grade 400 20M bars (cross-sectional area, 300 mm$^2$) were used as longitudinal steel, and grade 60 US No. 3 bars (cross-sectional area, 71 mm$^2$) were used for lateral reinforcement. According to standard A370 (ASTM 2000*a*), the yield stresses for these two bars were 402 and 500 MPa, respectively, with corresponding yield strains of 0.002102 and 0.00255. Clear concrete cover in the columns was 20 mm to the lateral steel and 30 mm to the longitudinal steel.

### Glass-fibre-reinforced polymer

Prefabricated GFRP shells were used as stay-in-place formwork for 11 specimens. This FRP system consisted of high-strength E-glass fibres embedded in an epoxy matrix. The GFRP shells, with various volumes and configurations or orientations of fibres, also acted as reinforcement for the columns, primarily for confining purposes. The thickness of one layer of GFRP in the shell was approximately 1 mm. The inner diameter of the shells was 356 mm. Eight coupons made of the material used for the GFRP shells were tested for tensile properties along the fibres according to standard D3039 (ASTM 2000*c*). The average tensile strength was 535 N/mm width of one layer of FRP, and the average rupture strain was 0.0237. The strength of eight specimens varied between 515 and 566 N/mm. The range of strain at rupture was 0.0217–0.0259.

### Construction of specimens

Ten reinforcement cages, approximately 1480 mm long and with a variety of steel arrangements, were constructed: (*i*) four cages consisted of six 20M longitudinal bars and No. 3 steel hoops at 320 mm spacing; (*ii*) three cages were constructed of six 20M longitudinal steel bars and No. 3 steel spirals with 75 mm pitch; and (*iii*) three cages had six

20M longitudinal steel bars and one No. 3 steel hoop at both ends to hold the bars together.

Six cylindrical sonotubes and 11 prefabricated GFRP shells were used to construct 17 column specimens. At each end of the 620 mm long test region in the middle of the tubes, four holes were drilled to carry two 6 mm diameter threaded rods in orthogonal directions through the tubes. These threaded rods were later used to install linear variable differential transducers (LVDTs). The bottoms of the tubes were sealed along their circumference with silicone to prevent leakage. A wooden bracing system was provided to support the tubes and keep them upright during casting. The forms were filled with concrete in three layers. Each layer was compacted with an internal rod vibrator. After casting, the specimens were covered with wet burlap and plastic sheets and cured for 3 d, after which the columns without FRP shells were stripped and all the columns were left for air curing. Nineteen cylinders cast with the columns were also covered with wet burlap and plastic for 3 d, after which they were stripped and left with the column specimens until testing.

A polyethylene sheet was applied inside the shells during their construction to provide a barrier between the GFRP and the concrete. The purpose of the polyethylene sheet was to protect the GFRP from chemically reacting with alkalis from the concrete. The barrier between GFRP and grout was considered necessary because, on the basis of simulated lab studies in which fibres alone were immersed in sodium hydroxide solution, researchers (Uomoto and Nishimura 1999) had reported that alkalis reacted adversely with glass fibres.

### Instrumentation

Instrumentation was provided to measure longitudinal column deformations, longitudinal steel bar strains, longitudinal GFRP strains, lateral steel strains, and lateral GFRP strains. The longitudinal column deformations of the test region of the specimens were recorded by four LVDTs (one each installed on the north, south, east, and west sides of the test region). These LVDTs were mounted vertically between the threaded rods that were installed in the specimens prior to casting. The gauge lengths of the LVDTs ranged between 610 and 620 mm.

Electric strain gauges were installed on the surface of the longitudinal and lateral steel. One strain gauge per longitudinal bar was installed at the centre of the bar, which was also the centre of the test region. The spirals with 75 mm pitch had four gauges at 90° from each other in the test region of the specimens. The specimens containing hoops at 320 mm had eight strain gauges: four on each of the two hoops in the test region. These strain gauges were also at 90° from each other on the periphery. Four strain gauges were attached externally on the surface of the GFRP shells to measure strains. Two of these strain gauges, at 180° to each other on the periphery, were used to measure longitudinal strains; the remaining two, also at 180° to each other, were used to measure lateral strains.

### Testing

The specimens were tested under monotonically increasing axial compression. Every effort was made to centre and align the specimens in the testing machine to ensure concentric loading. Plaster was used at the top and bottom ends of specimens in thin layers to ensure uniform application of the load. A 25.4 mm thick plate with a diameter of 343 mm was placed on the top of the specimen during testing, which further ensured uniform loading and avoided direct loading of the GFRP shell. To ensure that the failure would occur in the central test region of 620 mm, extra layers of GFRP were added in the end regions (above and below the test region) of the specimens before testing. A high-speed data acquisition system configured to read 100 sets of readings per second was used to record measurements from the load cell, strain gauges, and LVDTs. All the specimens were tested up to failure. The duration of the tests between the start of loading and the termination of the test varied between 5 and 20 min. The strain rate in the beginning of the test was about 0.001/min and increased to about 0.003/min in ductile columns beyond a strain of about 0.01.

## Results

Significant results from the tests are summarized in Table 3. The average strain obtained from the LVDT data and the stresses calculated from the applied loads were used to plot the response curves for all the specimens.

The contribution of the concrete in carrying the load was calculated by subtracting the longitudinal steel contribution from the total applied load at a particular strain level (Fig. 1*a*). For this calculation it was assumed that the strain in the concrete was equal to the strain in the longitudinal steel and that the strain was uniform over the gauge length. This was supported by the observation that the plots of total applied load versus longitudinal steel strains as measured by the strain gauges were in good agreement with the plots of total applied load versus column strains calculated from LVDT readings. In specimens confined with transverse steel but without GFRP shells, the cover in normal strength concrete columns starts to spall off at a strain of about 0.0015, and at a strain of approximately 0.0035 the cover is no longer effective in carrying the load (Sheikh and Uzumeri 1980). Between these two strain values, the effective area of concrete changes from the total column concrete area to the core concrete area. If linear variation is assumed for the effective concrete area, the confined concrete stress strain response can be determined as shown in Fig. 1*b*. The following parameters were calculated from the stress–strain curves for column concrete:

### Strength enhancement

Strength enhancement of all the columns was calculated using two different expressions (Sheikh and Uzumeri 1980):

$$[1] \qquad K_1 = f_{\mathrm{ccmax}} / 0.85 f'_{\mathrm{c}}$$

$$[2] \qquad K_2 = f_{\mathrm{ccmax}} / f'_{\mathrm{c}}$$

where $K_1$ is strength enhancement with respect to column concrete strength; $K_2$ is strength enhancement with respect to cylinder concrete strength; $f_{\mathrm{ccmax}}$ is maximum confined concrete stress; and $f'_{\mathrm{c}}$ is the unconfined concrete strength obtained from standard cylinder tests.

**Table 1.** Summary of column tests.

| Researcher | No. | Column size, $D{\times}L$ (mm) | $f_{co}'$ (MPa) | FRP properties: Type[a] | FRP properties: Total thickness (mm) | FRP properties: Tensile strength (MPa) |
|---|---|---|---|---|---|---|
| Ahmad et al. (1991) | 9 | 102×203 | 39.0–64.2 | Glass Fiber filament | $d$ = 1 mm | 2070 |
| Berthet et al. (2004) | 48 | 70×140 | 25–169.7 | C-wrap | 0.11–1.32 | 2500 |
| | | 160×320 | 25–169.7 | G-wrap | 0.11–1.32 | 3200 |
| Cairns and Sheikh (2001) | 8 | 356×1524 | 29.8 | C-tube | 0.5–1.0 | 1770 |
| Carey and Harries (2005) | 5 | 152×305 | 33.5 | C-wrap | 0.2 | 3500 |
| | | 254×762 | 38.9 | C-wrap | 1 | 875 |
| Demers and Neale (1994) | 8 | 152×305 | 32.2 | G-wrap | 0.3–1.05 | 629 |
| | | 152×305 | 43.7 | C-wrap | 0.3–1.05 | 1270 |
| Demers and Neale (1999) | 8 | 300×1200 | 20.5–47.7 | C-wrap | 0.9 | 1270 |
| Harries and Kharel (2003) | 50 | 152×305 | 32.1 | C-wrap, G-tube | 1–15 layers | 75–174 N/mm/ply |
| Jaffry and Sheikh (2001) | 8 | 356×1524 | 29.8 | G-tube | 1.0–2.0 | 535 |
| Karabinis and Rousakis (2002) | 16 | 200×320 | 34.8, 39.7 | C-wrap | 0.117–0.351 | 3720 |
| Karbhari and Gao (1997) | 24 | 152×305 | 18, 38.4 | C- and (or) G-wrap | 0.33–5.31 | 513–1353 |
| Kestner et al. (1997) | 32 | 152×610 | 26.2 | G-wrap, C-wrap | 0.165–1.728 | 382–4054 |
| | 3 | 508×1830 | 32.8 | G-wrap | 2.81 | 407 |
| | | 508×1830 | 32.8 | C-wrap | 3.05 | 569 |
| Kshirsagar et al. (2000) | 9 | 102×204 | 38–39.5 | G-wrap | 1.42 | 363 |
| Lin and Li (2003) | 81 | 100×200 | 17.2–27.5 | C-wrap | 0.11–0.33 | 4170 |
| | | 150×500 | 17.2–27.5 | C-wrap | 0.11–0.33 | 4170 |
| Lin and Liao (2004) | 6 | 100×200 | 23.9 | G-wrap | 1.84, 3.89 | 455.4–403 |
| Mandal et al. (2005) | 43 | 100×200 | 30.7–80.6 | G-wrap | 1.0–2.5 | 575 |
| | | 100×200 | 30.7–80.6 | C-wrap | 1.0–2.5 | 784 |
| Mastrapa (1997) | 10 | 153×310 | 29.8, 31.2 | G-wrap | 0.61–3.07 | 565 |
| Matthys et al. (1999) | 12 | 150×300 | 34.9 | C-wrap | 0.12, 0.24 | 1100, 2600 |
| Mirmiran et al. (1998) | 38 | 153×305 | 29.6–44.8 | G-tube | 1.45–2.97 | 524–641 |

| Results | | | | | |
|---|---|---|---|---|---|
| Stiffness (MPa) | $f_{ccmax}/f_{co}'$ | $\varepsilon_{cc}/\varepsilon_{co}$ | Post-peak curve[b] | Type of response | Remarks |
| 48 300 | 2.27 | 4.556–5.136 | Y | Regular curve | Parabolic curve segment with post-peak behaviour; fracture of filament did not cause sudden release of energy at peak load, which led to the post-peak behaviour |
| 74 000 | 1.09–4.15 | 1.73–12.5 | N | Bilinear curves | Gain in strength and ductility due to FRP confinement decreased with an increase in concrete strength |
| 230 000 | 1.09–4.15 | 1.73–12.5 | N | Bilinear curves | Gain in strength and ductility due to FRP confinement decreased with an increase in concrete strength |
| 82 326 | 1.46–1.99 | 4.94–9.61 | Y | Ductile post-peak behaviour | Progressive failure of FRP gradually released energy and resulted in very ductile post-peak behaviour |
| 250 000 | 1.40–1.41 | 3.47–4.04 | N | Bilinear curves | |
| 72 500 | 1.40–1.41 | 3.47–4.04 | N | Bilinear curves | |
| 30 000 | 0.96–1.72 | 1.04–8.21 | N | Bilinear curves | |
| 84 000 | 0.96–1.72 | 1.04–8.21 | N | Bilinear curves | |
| 84 000 | 1.10–1.53 | 1.36–4.46 | Y | Mostly trilinear response | Two ascending branches followed by a descending branch; large-scale specimens normally exhibited post-peak behaviour |
| 4 900 – 15 700 N/mm/ply | 1.02–1.87 | 0.75–4.93 | N | Mostly bilinear curves | Specimens with low confinement showed behaviour similar to that for unconfined concrete or displayed short, horizontal post-peak response |
| 22 574 | 1.09–1.84 | 2–9.68 | Y | Mostly trilinear response | Large-scale specimens displayed post-peak ductile response; see remarks for Cairns and Sheikh (2001) for details |
| 240 000 | 1.08–1.94 | 1.26–8.99 | S | Mostly bilinear response | Only one LVDT was used for longitudinal strain, and most specimens bent to LVDT side at failure |
| 35 856 – 150 150 | 1.17–4.57 | NA | N | Bilinear curves | For some wraps, only total thickness of FRP wraps was given |
| 16 551 – 176 364 | 1.46–2.49 | 6.19–8.91 | N | Bilinear curves | |
| 20 216 | 1.09 | 3.9 | Y | Trilinear curves | Transverse steel in addition to FRP may contribute to post-peak descending branch; CFRP-wrapped columns were less ductile than GFRP-wrapped columns |
| 38 684 | 1.52 | 5.65 | Y | Trilinear curves | Transverse steel in addition to FRP may contribute to post-peak descending branch; CFRP-wrapped columns were less ductile than GFRP-wrapped columns |
| 19 900 | 1.50–1.60 | 7.28–8.14 | N | Bilinear curves | |
| 232 000 | 1.72–5.23 | NA | NA | NA | |
| 232 000 | 1.72–5.23 | NA | NA | NA | |
| 22 458 – 23 825 | 2.60–3.92 | NA | N | Bilinear curves | |
| 26 100 | 1.17–2.58 | 1.33–11.41 | N | Bilinear curves | |
| 47 000 | 1.17–2.58 | 1.33–11.41 | N | Bilinear curves | |
| 19 185 | 1.13–3.11 | NA | N | Mostly bilinear response | Specimens with low confinement displayed descending branch after peak load followed by increase in load up to failure; failure load was lower than peak load |
| 420 000, 200 000 | 1.17–1.32 | 1.71–4.05 | N | Bilinear curves | |
| 37 233 – 40 749 | 1.09–3.88 | 4.81–20.35 | N | Bilinear curves | |

**Table 1** (*concluded*).

| | | | | FRP properties | | |
|---|---|---|---|---|---|---|
| Researcher | No. | Column size, $D \times L$ (mm) | $f_{co}'$ (MPa) | Type[a] | Total thickness (mm) | Tensile strength (MPa) |
| | | 153×610 | 29.6–44.8 | G-tube | 1.45–2.97 | 524–641 |
| Miyauchi et al. (1997) | 28 | 150×300 | 23.6–51.9 | C-wrap | 0.11–0.33 | 3481 |
| Nanni and Bradford (1995) | 19 | 150×300 | 36.3 | G-wrap | 0.3–4.3 | 583 |
| | | 150×300 | 35.6 | A-wrap | 0.3–4.3 | 1150 |
| Purba and Mufti (1999) | 1 | 190.6×787.9 | 27.06 | C-wrap | 0.22 | 3483 |
| Saffi et al. (1999) | 18 | 152×435 | 35 | G-wrap, C-wrap | 0.11–2.4 | 450–3700 |
| Shahawy et al. (2000) | 45 | 152.5×305 | 19.4, 49 | C-wrap | 0.5–2.5 | 2275 |
| Soudki and Green (1996) | 6 | 152×305 | 36 | C-wrap | 0.16–0.32 | 1481 |
| Theriault et al. (2004) | 24 | 51×102 | 18–39 | C-wrap | 0.165–3.9 | 3327 |
| | | 304×1824 | 18–39 | G-wrap | 0.165–3.9 | 493.8 |
| Toutanji (1999) | 12 | 76×305 | 31 | G-wrap, C-wrap | 0.22–0.33 | 1518–3485 |
| Toutanji and Deng (2002) | 4 | 76×305 | 44 | A-wrap | 0.573 | 2059 |
| Watanabe et al. (1997) | 27 | 100×200 | 30.2 | A-wrap, C-wrap | 0.089–0.427 | 2452–3432 |
| Xiao and Wu (2000) | 27 | 152×305 | 33.7–55.2 | C-wrap | 0.38–1.14 | 1577 |
| Zhang et al. (2000) | 5 | 150×30 | 34.3 | C-wrap | 1 | 753 |

**Note:** LVDT, linear variable differential transducer; NA, not available.

[a]A-wrap, aramid-fibre-reinforced-polymer wrap; C-tube, carbon-fibre-reinforced-polymer (CFRP) tube; C-wrap, CFRP wrap; G-tube, glass-fibre-reinforced-

[b]N, not existing (i.e., post-peak behaviour does not exist or is not presented); S, sometimes existing (i.e., some of the curves appear to have post-peak peak behaviour exists and is presented).

**Table 2.** Details of test specimens.

| | | Lateral steel | | | | Longitudinal steel | |
|---|---|---|---|---|---|---|---|
| Spec. No. | Specimen designation | Size (US No.) | Spacing (mm) | Volumetric ratio, $\rho_s$ (%) | No. of bars | Size (No.) | Volumetric ratio, $\rho_l$ (%) |
| 1 | 00-10-1 | — | — | — | 1 | 20M | 0.30 |
| 2 | 00-10-2 | — | — | — | 1 | 20M | 0.30 |
| 3 | 00-LS320-3 | 3 | 320 | 0.289 | 6 | 20M | 1.81 |
| 4 | 00-LS320-4 | 3 | 320 | 0.289 | 6 | 20M | 1.81 |
| 5 | 00-LS75-5 | 3 | 75 | 1.230 | 6 | 20M | 1.81 |
| 6 | 00-LS75-6 | 3 | 75 | 1.230 | 6 | 20M | 1.81 |
| 7 | G01-00-7 | — | — | — | — | — | — |
| 8 | G11-00-8 | — | — | — | — | — | — |
| 9 | G01-L0-9 | — | — | — | 6 | 20M | 1.81 |
| 10 | G01-LS320-10 | 3 | 320 | 0.289 | 6 | 20M | 1.81 |
| 11 | G02-00-11 | — | — | — | — | — | — |
| 12 | G22-00-12 | — | — | — | — | — | — |
| 13 | G02-L0-13 | — | — | — | 6 | 20M | 1.81 |
| 14 | G02-LS320-14 | 3 | 320 | 0.289 | 6 | 20M | 1.81 |
| 15 | G02-LS75-15 | 3 | 75 | 1.230 | 6 | 20M | 1.81 |
| 16 | G45°2-00-16 | — | — | — | — | — | — |
| 17 | G45°2-L0-17 | — | — | — | 6 | 20M | 1.81 |

**Note:** $\rho_s$, volumetric ratio of lateral steel to concrete core; $\rho_l$, ratio of area of longitudinal steel to that of cross section.

## Ductility

A ductility factor ($\mu$) for the specimens was calculated using the following relationship:

$$[3] \qquad \mu = \varepsilon_2 / \varepsilon_0$$

where $\varepsilon_0$ is the axial strain corresponding to the maximum confined concrete stress ($f_{ccmax}$) on the initial tangent ($E_t$); and $\varepsilon_2$ is the axial strain corresponding to a strength of $0.8 f_{ccmax}$ on the descending portion of the stress–strain curve (Fig. 2). A 20% drop in strength is generally used to evaluate the deformability of structural components (Sheikh and Uzumeri 1980). In addition, the concrete stress–strain curve is needed up to this point for a member analysis under axial load and flexure.

| Results | | | | | |
|---|---|---|---|---|---|
| Stiffness (MPa) | $f_{ccmax}/f_{co}'$ | $\varepsilon_{cc}/\varepsilon_{co}$ | Post-peak curve[b] | Type of response | Remarks |
| 37 233 – 40 749 | 1.09–3.88 | 4.81–20.35 | N | Bilinear curves | |
| 230 500 | 1.31–3.26 | 4.32–13.2 | N | Bilinear curves | |
| 52 000 | 1.13–6.85 | $\varepsilon_{co}'$ NA | N | Bilinear curves | |
| 62 200 | 1.13–6.85 | $\varepsilon_{co}'$ NA | N | Bilinear curves | |
| 230 535 | 1.99 | 2.9 | N | Bilinear curves | |
| 36 000 – 415 000 | 1.51–2.77 | 4–11.48 | N | Bilinear curves | |
| 82 700 | 1.21–4.13 | 3.1–17.8 | N | Bilinear curves | |
| 140 000 | 1.47–1.64 | 3.07–3.72 | N | Bilinear curves | Ascending branch was somewhat horizontal with a slight increase in strength; this might be due to low confinement from FRP |
| 230 000 | 1.73–3.89 | NA | N | Bilinear curves | |
| 27 600 | 1.73–3.89 | NA | N | Bilinear curves | 6 of specimens with diameter of 304 mm |
| 72 600 – 372 800 | 1.96–3.06 | 8.053–12.89 | N | Bilinear curves | |
| 118 000 | 3.42 | 10.08 | N | Bilinear curves | |
| 73 000 – 628 600 | 1.29–3.46 | 2.5–24.1 | N | Bilinear curves | |
| 105 000 | 1.05–2.83 | 1.12–12.0 | N | Bilinear curves | |
| 91 000 | 1.73 | 3.704 | N | Bilinear curves | |

polymer (GFRP) tube; G-wrap, GFRP wrap.
behaviour; however, this might not be reliable, as only one LVDT was applied to measure the longitudinal strains of specimens); Y, existing (i.e., post-

**Table 3.** Results from the experimental program.

| Spec. No. | Name | $P_{max}$ (kN) | $f_{ccmax}$ (MPa) | $\varepsilon_{cc}$ (mm/mm) | Conf. pressure (MPa) | $K_1$ | $K_2$ | μ | $e_{80}$ | $e_{50}$ | $W_{80}$ | $W_{50}$ |
|---|---|---|---|---|---|---|---|---|---|---|---|---|
| 1 | 00-10-1 | 3125 | 30.7 | 0.001 40 | 0.000 | 1.20 | 1.02 | 3.19 | 0.081 | NA | 2.52 | NA |
| 2 | 00-10-2 | 3350 | 32.5 | 0.002 34 | 0.000 | 1.28 | 1.08 | 3.98 | 0.118 | NA | 3.27 | NA |
| 3 | 00-LS320-3 | 3130 | 25.9 | 0.001 70 | 0.350 | 1.01 | 0.86 | 4.92 | 0.092 | 0.122 | 4.02 | 5.35 |
| 4 | 00-LS320-4 | 3665 | 30.1 | 0.002 11 | 0.350 | 1.18 | 1.00 | NA | NA | NA | NA | NA |
| 5 | 00-LS75-5 | 4125 | 44.0 | 0.004 00 | 2.768 | 1.73 | 1.47 | 9.27 | 0.513 | 0.936 | 7.75 | 14.15 |
| 6 | 00-LS75-6 | 4030 | 44.0 | 0.004 62 | 2.768 | 1.73 | 1.47 | 10.26 | 0.584 | 0.900 | 8.84 | 13.62 |
| 7 | G01-00-7 | 3460 | 34.8 | 0.003 70 | 3.014 | 1.36 | 1.16 | 9.08 | 0.336 | 0.517 | 8.14 | 12.53 |
| 8 | G11-00-8 | 3820 | 38.4 | 0.004 03 | 3.014 | 1.51 | 1.28 | 8.57 | 0.390 | 0.500 | 7.75 | 9.93 |
| 9 | G01-L0-9 | 3895 | 32.4 | 0.007 39 | 3.014 | 1.27 | 1.08 | 10.81 | 0.350 | 0.490 | 9.75 | 13.65 |
| 10 | G01-LS320-10 | 4360 | 37.2 | 0.011 51 | 3.364 | 1.46 | 1.24 | 14.30 | 0.580 | 0.680 | 12.29 | 14.41 |
| 11 | G02-00-11 | 4460 | 44.8 | 0.011 99 | 6.028 | 1.76 | 1.49 | 13.56 | 0.817 | 1.186 | 11.92 | 17.30 |
| 12 | G22-00-12 | 5450 | 54.8 | 0.009 79 | 6.028 | 2.15 | 1.83 | 14.16 | 1.320 | 1.528 | 12.90 | 14.93 |
| 13 | G02-L0-13 | 5500 | 48.9 | 0.012 51 | 6.028 | 1.92 | 1.63 | 10.87 | 1.160 | 1.560 | 14.24 | 19.15 |
| 14 | G02-LS320-14 | 5570 | 49.3 | 0.017 92 | 6.378 | 1.93 | 1.64 | 15.49 | 1.070 | 1.570 | 12.89 | 18.92 |
| 15 | G02-LS75-15 | 6020 | 54.0 | 0.016 72 | 8.796 | 2.12 | 1.80 | 16.49 | 1.420 | 2.100 | 14.27 | 21.10 |
| 16 | G45°2-00-16 | 3740 | 37.6 | 0.001 93 | 8.439 | 1.47 | 1.25 | 13.93 | 0.610 | 1.070 | 12.64 | 22.18 |
| 17 | G45°2-L0-17 | 4250 | 36.1 | 0.009 15 | 8.439 | 1.42 | 1.20 | 38.41 | 1.600 | 1.830 | 35.95 | 41.12 |

**Note:** NA, not available.

## Energy capacity

The energy capacity ($e_i$) is defined as the area under the concrete stress–strain curve up to $i$% of $f_{ccmax}$ and·is given in newton millimetres per cubic millimetre. The energy capacity values were calculated for three levels of stress, which were used to provide a wide spectrum of specimen behaviour along the descending branch of the curve. The first was the area under the stress–strain curve up to 80% of $f_{ccmax}$ on the descending portion of the curve; the second, the area up to 50% of $f_{ccmax}$; and the third, the area up to 20% of $f_{ccmax}$. These were denoted as $e_{80}$, $e_{50}$, and $e_{20}$, respectively, and are also shown in Fig. 2.

**Fig. 1.** Concrete contribution curves.

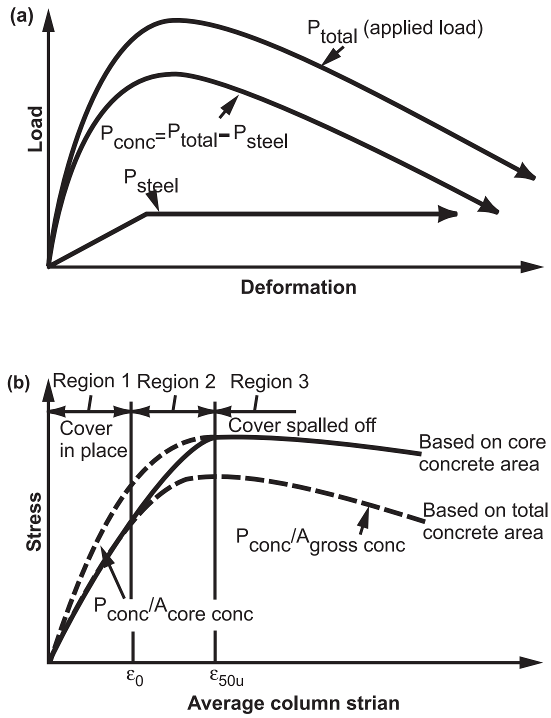


**Fig. 2.** Typical confined concrete stress–strain curve.

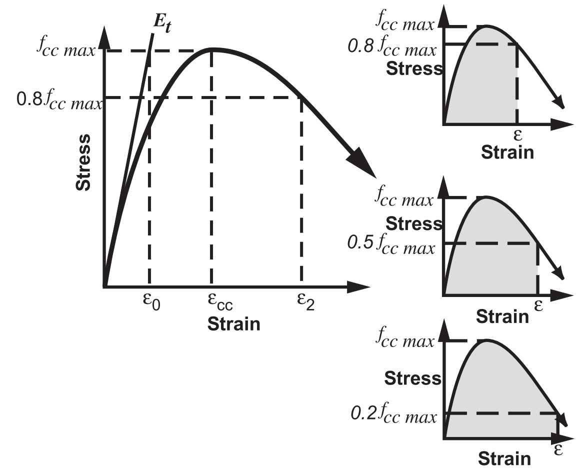


## Work index

The energy capacity calculated was normalized to obtain a dimensionless parameter termed the work index ($W_i$). The following expression was used to normalize the area under the stress–strain curve:

$$[4] \qquad W_i = e_i/(f_{\mathrm{ccmax}}\varepsilon_0)$$

## Test observations

The testing procedure included inspecting and monitoring the specimens to characterize their failure tendencies and behaviour. It is important to mention here that all the specimens failed within the test region, that is, within the LVDT gauge length. For the six control specimens without any GFRP shell, the first signs of distress appeared as vertical cracks within the test region at their mid-heights. For the plain concrete columns (specimens 1 and 2), the failure was a sudden burst of the test region immediately after the development of vertical cracks around the entire circumference of the specimens. Specimens 3 and 4, with hoops at 320 mm spacing, had minimal confinement. These specimens failed suddenly as the cover spalled off, followed by an abrupt outburst of the core and buckling of the longitudinal steel.

Vertical cracks developed symmetrically around the entire central region in specimens 5 and 6, in which the core concrete was confined with spirals at 75 mm pitch. With increasing load, the cracks increased in size and number until the cover concrete started to spall off. Because of the confinement provided by the spiral, the core concrete did not experience the same lateral deformation as encountered by the cover. As a result, under incremental loading the core expanded laterally outward against the lateral and longitudinal steel. Meanwhile, the longitudinal steel began to buckle and further pushed against the lateral steel. Finally the failure of the specimens was accompanied by the crushing of the core concrete. The spirals were found to rupture at more than one location in both specimens.

All the specimens with GFRP shells failed in a similar fashion, except specimens 16 and 17, which contained fibres at an inclination of 45°. The failure, in general, was marked by rupture of the GFRP shell in the test region. The rupture of the shell was found to start at one location and moved around the circumference, accompanied by irregular exploding sounds. The specimens exhibited considerable ductile behaviour, which was also accompanied by sufficient warning before failure. Figure 3 shows a few representative specimens at the end of the tests.

Specimen 13, with two layers of GFRP in the shell, did not perform as well as expected. Although every effort was made to apply loads concentrically, this specimen was inadvertently subjected to eccentric loading and experienced bending about the east–west axis, causing additional compression on its south side. Specimens 16 and 17, with fibres inclined at 45° to the horizontal, behaved in a more ductile manner than other columns. They did not burst out, and the FRP did not rip off as in other columns. Instead, these specimens settled down softly and displayed a rupture plane inclined at an angle of about 45°.

# Discussion

## Effect of number of layers of glass-fibre-reinforced-polymer shells

### *Specimens with no longitudinal or lateral steel*

Figure 4*a* shows the stress–strain responses of concrete in four specimens without any longitudinal or lateral steel. Specimens 1 and 2 had no confining reinforcement, and specimens 7 and 11 had GFRP shells with one and two layers of glass fibres, respectively. The addition of one layer of GFRP confinement to concrete increased its strength by more than 10%, whereas the confinement provided by two layers of GFRP increased the strength to approximately 42% (Table 2). Ductility factor ($\mu$), energy capacity ($e_i$), and work index ($W_i$) improved considerably more. The ductility factor ($\mu$) and work index ($W_{80}$) corresponding to a 20% drop in stress beyond the peak increased by a factor of approxi-

**Fig. 3.** Selected specimens after testing.

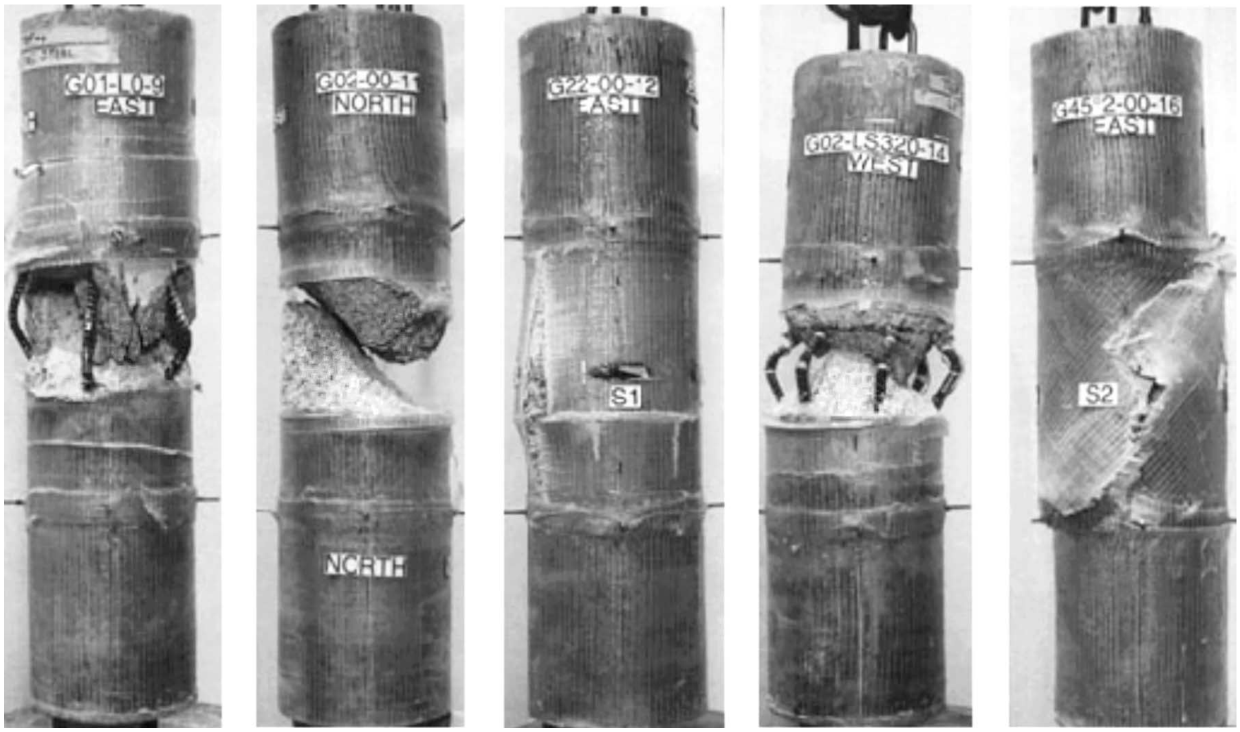


G01-L0-9 G02-00-11 G22-00-12 G02-LS320-14 G45-2-00-16

mately four as a result of two layers of GFRP in the transverse direction, and the energy capacity improved by more than eight times. The corresponding increases with one layer of GFRP were in the range of 250%–340%. Improvements in the total energy capacity corresponding to failure were even more significant. An increase in concrete strength due to one layer of GFRP was less than half that obtained by two layers. This was also observed in comparisons of other pairs of specimens, such as specimen 9 versus specimen 13; and specimen 10 versus specimen 14. It appears that one layer of GFRP is not stiff enough to produce a sufficiently large confining pressure at reasonably small lateral strains in the concrete. By the time GFRP is able to apply significant confining pressure, the lateral strain in the concrete is too large for the confining pressure to effectively enhance its compressive strength.

### *Specimens with longitudinal steel and hoops at 320 mm spacing*

Figure 4*b* shows the concrete behaviour in three specimens, each containing six 20M longitudinal steel bars and having hoops at 320 mm spacing. Specimen 3 had no GFRP shell, whereas specimens 10 and 14 had GFRP shells with one and two layers of fibres in the circumferential direction, respectively. The ductility factor of the concrete increased from 4.9 to 14.3 as a result of the confinement provided by one layer of GFRP and increased to 15.5 with two layers of GFRP. It can also be observed that the energy capacity ($e_{80}$) increased by more than 500% as a result of using a one-layered GFRP shell (specimen 10 versus specimen 3). The energy capacity almost doubled again with the addition of one more GFRP layer (specimen 14 versus specimen 10). The strength of concrete increased by about 33% and 76% as a result of confinement provided by one and two layers of GFRP, respectively. Results from both specimens 3 and 4 were used to calculate the average response of the unconfined concrete.

In specimens containing longitudinal steel and hoops at 320 mm spacing, the improvements in concrete properties due to GFRP shells were superior to those observed in specimens without any steel reinforcement. The confinement provided by the longitudinal steel and the hoops is more efficient in the presence of GFRP shell, which prevents spalling of the concrete cover and buckling of the longitudinal bars until the rupture of the glass fibres. By keeping the column intact, GFRP allows the steel reinforcement to be fully utilized in carrying the axial load and confining the concrete.

### *Specimens with longitudinal steel and spirals at 75 mm pitch*

A comparison of specimens 1, 2, 5, 6, and 15 shows the effects of steel spiral and GFRP shell on the behaviour of columns (Table 3; Fig. 4*c*). Specimens 1 and 2 represented unconfined concrete behaviour, while specimens 5 and 6 were reinforced with six 20M longitudinal steel bars and spirals with 75 mm pitch in accordance with the provisions of the ACI (1999) and CSA (1994) codes. Specimen 15 had a two-layered GFRP shell, in addition to the same steel reinforcement as specimens 5 and 6 had. Confinement provided by the spiral steel improved the behaviour of concrete in a significant manner, showing increases in strength, ductility factor (μ), and energy capacity ($e_{80}$) of approximately 40%, 170%, and 450%, respectively (specimens 5 and 6 versus

**Fig. 4.** Comparison of axial stress – axial strain responses for (*a*) specimens with no longitudinal or lateral steel, (*b*) specimens with longitudinal steel and lateral steel hoops at 320 mm spacing, (*c*) specimens with longitudinal steel and spiral at 75 mm pitch, (*d*) specimens with hoops at 320 mm and specimens with one-layer glass-fibre-reinforced-polymer (GFRP) shell, (*e*) specimens with spirals at 75 mm and specimens with two-layer GFRP shell, (*f*) specimens with two-layer GFRP shell.

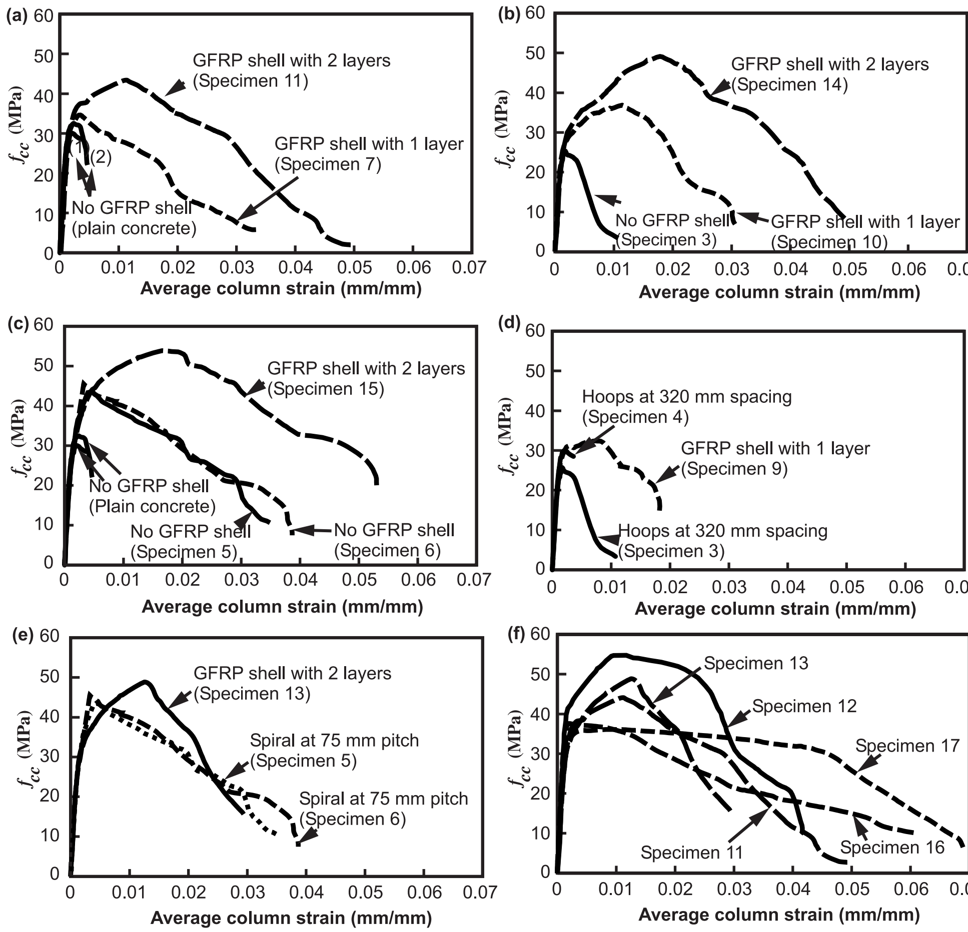


specimens 1 and 2). Additional confinement by two layers of GFRP further improved concrete behaviour such that the concrete strength was 71% higher than the unconfined strength; and the ductility factor and energy capacity increased by about 5 times and 14 times compared with the respective properties of unconfined concrete.

A comparison of specimens 5 and 6 with specimen 10 shows that hoops at 320 mm spacing plus one-layered GFRP shell can easily replace the steel spiral with 75 mm pitch and result in columns with equivalent ductile behaviour. Ductile columns designed according to the code provisions (CSA 1994; ACI 1999) would generally require closely spaced transverse reinforcement, which may be difficult to accommodate during construction. The use of GFRP shells for confinement reinforcement and stay-in-place forms will allow larger spacing of transverse steel reinforcement while producing ductile performance in columns. This is further discussed in the next section.

### Confinement by glass-fibre-reinforced-polymer shells versus confinement by lateral steel

A comparison is made between specimens 3, 4, 5, 6, 9, and 13. These specimens are similar in every respect except that specimens 3, 4, 5, and 6 are confined with lateral steel, whereas specimens 9 and 13 are confined with GFRP shells. The purpose of this comparison is to evaluate the potential of GFRP shells to replace the conventional steel for lateral reinforcement. A comparison of specimens 3, 4, and 9 shows that one layer of GFRP shell can safely replace lateral steel at 320 mm spacing (Fig. 4*d*). The total load-carrying capacity, the ductility factor, the energy capacity, and the work index of specimen 9 with a GFRP shell are all significantly higher than those of specimens 3 and 4 with hoops at 320 mm (Table 3). In fact, the values for these parameters are approximately equal to those of specimens 5 and 6, which contained spirals at 75 mm pitch (Table 3). The values for all the strength and ductility parameters are higher for specimen 13, with two layers of GFRP shells, than for specimens 5 and 6 (Fig. 4*e*; Table 3). As described earlier, specimen 13 did not perform as well as expected, because of the inadvertent eccentricity of the applied load. Thus, a column with no lateral steel and confined with two layers of GFRP shells would exhibit much better performance than a column confined with spirals at 75 mm spacing.

### Specimens confined with fibres inclined at 45°

Figure 4*f* shows the responses of specimens 16 and 17. Each of these specimens contained no lateral steel and used a GFRP shell made of two layers of glass fibres, one oriented at +45° and the other at –45°. Specimen 16 contained no longitudinal steel, whereas specimen 17 had six steel bars. These specimens were comparable to specimens 11, 12, and 13 (also included in Fig. 4*f*) except for the orientation of the fibres. The specimens with 45° fibre orientation displayed a much smaller strength gain (20%–25%) than specimens with fibres oriented in the transverse direction (49%–82%). As shown in Table 3, the values of the ductility factor, energy capacity, and work indices for specimen 17 were significantly higher than those for the other four specimens. Work indices of specimen 16 were also higher than those of the comparable specimens 11 and 12. Although the 45° fibres were not very effective in enhancing the strength of concrete, they improved the deformability of concrete much better than the transverse fibres did. This indicated a softer response of the 45° fibres compared with that of transverse fibres under the influence of lateral pressure generated by the expanding concrete. This observation is similar to that made by Howie and Karbhari (1995) about the gentle failure of FRP jackets with fibres oriented in +45° and –45° directions.

To investigate this further, one GFRP coupon of dimensions 127 mm × 432 mm was cut from the shell of specimens 16 after its testing. The coupon comprised two grips, each of 152.5 mm length, and a test region of 127 mm length. The tensile behaviour of the coupon from specimen 16 is shown in Fig. 5, along with a photo of the failed coupon. Also shown in the figure is the tensile force – strain response based on a 127 mm wide single-layered GFRP coupon with fibres oriented in the direction of the applied load. The failure loads from the two tests were comparable, but the 45° coupon had approximately 41% more area in the direction of the load. In addition, the 45° coupon initially displayed a stiff behaviour, but in the later stages a softer and more ductile behaviour was observed. The tensile behaviour of the two coupon specimens partly explains the lower strength and higher ductility of specimens 16 and 17. Further experimental work is needed to study the behaviour of columns reinforced with fibres oriented at 45°.

**Fig. 5.** Tensile properties of glass-fibre-reinforced polymer. Note: LVDT, linear variable differential transducer.

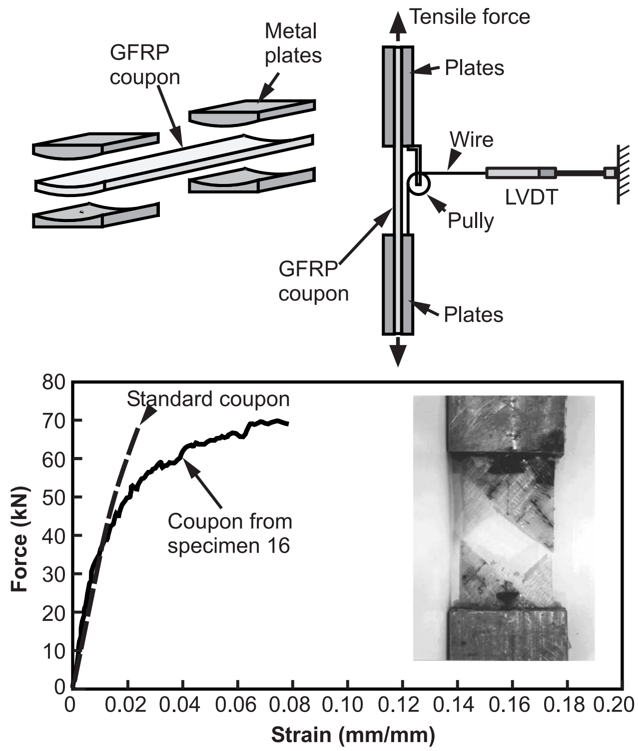


**Fig. 6.** Effect of longitudinal fibres on column behaviour.

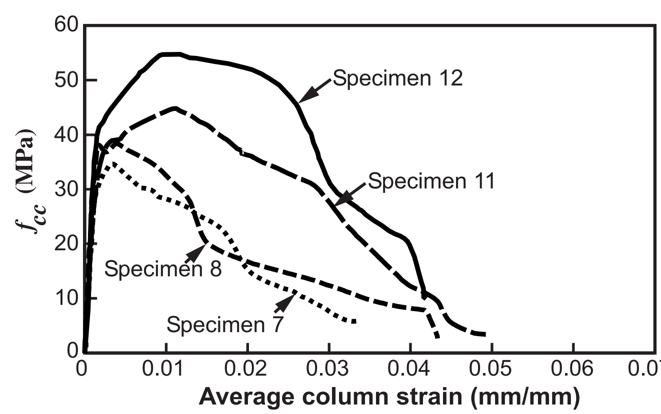


## Effect of longitudinal fibres on column behaviour

The effect of the longitudinal fibres on the behaviour of GFRP-encased columns can be examined by considering the responses of specimens 7 and 8 and of specimens 11 and 12 (Fig. 6). The only difference between specimens 7 and 8 is the presence of one layer of longitudinal fibres in specimen 8. Similarly, specimens 11 and 12 are identical except for the presence of two layers of longitudinal glass fibres in specimen 12. None of these specimens contained any steel reinforcement. The contribution of the longitudinal glass fibres was not subtracted from the total load in the determination of the stress–strain curves shown in Fig. 6. It can be observed from the two sets of specimens that glass fibres in the longitudinal direction contributed significantly toward the load-carrying capacity of the columns. One layer of longitudinal fibres increased column capacity by about 10% (specimens 7 and 8), while with two layers of the longitudinal fibres, the strength increase was about 22% (specimens 11 and 12). The longitudinal glass fibres did not have any significant effect on ductility factors and work indices. The energy capacities of specimens, however, improved with the addition of the longitudinal fibres, primarily as a result of the higher strength. The improvement in the load-carrying capacity of specimens with one layer of longitudinal glass fibres was 360 kN; it was 990 kN when two layers of longitudinal fibres were used. The tensile capacity of one layer of longitudinal FRP, considering average fibre strength, is 598 kN. The fibres were reasonably effective in carrying the compressive load as an integral part of the concrete–fibre composite. Despite the presence of a polyethylene sheet separating the concrete and the FRP shell, expansion of concrete due to Poisson's effect engaged the longitudinal fibres in the axial direction to participate in carrying the load.

**Behaviour of fibre-reinforced polymer in columns**

Results from the tests presented here show that FRP-confined concrete displays a response that includes a stable descending branch. It was observed during the tests that the fibres in the test region did not all rupture at once. Crackling sounds of progressive fibre rupture began when the fibre strains were about half the rupture values. The peak load-carrying capacity of the concrete generally occurred around the start of the fibre rupture or soon after, but this did not represent the ultimate failure of the column. Progressive rupture of fibres beyond this point resulted in softening of concrete, which provided the descending part of its stress–strain response.

In Fig. 7, typical idealized FRP behaviour is shown from the origin to point A. If the initiation of rupture in some fibres starts at $\varepsilon = a\varepsilon_{rup}$ $(0 < a < 1)$, the FRP response will start deviating from the ideal behaviour at point B. The total force in FRP at final rupture (point C) will be $bF_u$, where $b$ is the fraction of intact fibres at that stage. The shape of the curve between B and C will depend on the nature of the progressive failure of fibres. With this force–strain relationship of FRP, the confining pressure on the concrete does not decrease from the maximum value to zero with a sudden drop and explains the softening of concrete at large strains and the presence of post-peak response (Punshi and Sheikh 2003). This effect will be more pronounced in large columns where a substantial length of FRP needs to rupture before the column completely loses its load-carrying capacity. In small specimens, only a small length of FRP needs to rupture before the specimen suddenly loses its strength. Data from 635 column specimens in Table 1 confirm this argument.

**Fig. 7.** Tensile characteristics of glass-fibre-reinforced polymer in coupons and in columns.

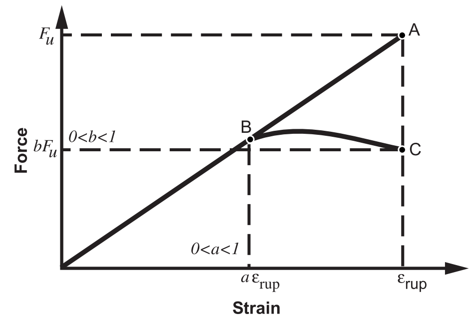


## Concluding remarks

Results from this experimental study on 17 columns of 356 mm diameter show that FRP shells can be used for stay-in-place formwork and effective confinement reinforcement for concrete columns. The shells also protect the encased concrete and steel against harsh environmental effects, such as salt attack. The additional expense of providing the shells can be offset partially by the savings realized by the elimination of the labour cost required to remove the traditional formwork and the need to provide closely spaced lateral steel reinforcement. Large spacing between the steel reinforcement would help improve the quality of cast-in-place concrete, in addition to improving the efficiency of the casting operation.

The following conclusions can be drawn from the results of this study:

(1) There was a significant increase in compressive strength, axial strain at peak stress, ductility, and energy capacity of concrete columns owing to the confinement provided by GFRP shells. Improvements in excess of 14 times were observed in the energy capacity of concrete.

(2) The behaviour of 356 mm diameter specimens with GFRP shells containing one layer of transverse fibres was significantly better than that of similar specimens with lateral steel placed at 320 mm spacing. Similarly, specimens with GFRP shells containing two layers of fibres in the transverse direction were superior to specimens containing spirals with 75 mm pitch.

(3) Fibres in the longitudinal direction enhanced the load-carrying capacity of the columns, but their improvement of the ductility parameters was minimal.

(4) Columns confined with both GFRP and lateral steel performed the best among all the specimens in the test series, indicating that the presence of GFRP shells enhances the contributions of steel reinforcement by delaying buckling of the longitudinal bars and preventing spalling of the concrete cover.

(5) Specimens with GFRP shells with fibres inclined at 45° displayed significantly more ductile behaviour than specimens containing equivalent fibre reinforcement in the longitudinal and transverse directions.

## Acknowledgments

The research reported here was supported by grants from the Natural Sciences and Engineering Research Council (NSERC) of Canada and ISIS Canada, an NSERC Network of Centres of Excellence. Financial and technical assistance from the Fyfe Co., of California, R.J Watson, Inc. of Amherst, New York, and Premier Corrosion of Oakville, Ontario, is gratefully acknowledged. Experimental work was carried out at the Structures Laboratories of the Department of Civil Engineering at the University of Toronto.

## References

ACI. 1999. Building code requirements for structural concrete (318-99) and commentary (318R-99). American Concrete Institute (ACI), Farmington Hills, Mich.

Ahmad, S.H., Khaloo, A.R., and Irshaid, A. 1991. Behaviour of concrete spirally confined by fibreglass filaments. Magazine of Concrete Research, **43**(156): 143–148.

ASTM. 2000*a*. Standard test methods and definitions for mechanical testing of steel products. Annual Book of ASTM Standards. Vol. 01.04. Standard A370-00. American Society for Testing and Materials (ASTM), West Conshohocken, Pa.

ASTM. 2000*b*. Standard test method for compressive strength of cylindrical concrete specimens. Annual Book of ASTM Standards. Vol. 04.02. Standard C39/C39M. American Society for Testing and Materials (ASTM), West Conshohocken, Pa.

ASTM. 2000*c*. Standard test method for tensile properties of polymer matrix composite materials. Annual Book of ASTM Standards. Vol. 15.03. Standard D3039-00. American Society for Testing and Materials (ASTM), West Conshohocken, Pa.

Azizinamini, A., Corley, W.G., and Johal, L.S.P. 1992. Effects of transverse reinforcement on seismic performance of columns. ACI Structural Journal, **89**(4): 442–450.

Berthet, J.F., Ferrier, E., and Hamelin, P. 2004. Compressive behavior of concrete externally confined by composite jackets. Part A: Experimental study. Construction and Building Materials, **19**: 223–232.

Cairns, S.W., and Sheikh, S.A. 2001. Circular concrete columns externally reinforced with pre-fabricated carbon polymer shells. Department of Civil Engineering, University of Toronto, Toronto, Ont. Research Report SC-01-01.

Carey, S.A., and Harries, K.A. 2005. Axial behavior and modeling of confined small-, medium- and large-scale circular sections with carbon fiber-reinforced polymer jackets. ACI Structural Journal, **102**(4): 596–604.

Considère, A. 1903. Experimental research on reinforced concrete. Translated and arranged by L.S. Moisseiff. McGraw Publishing Co., New York, N.Y. 188 p.

CSA. 1994. Design of concrete structures. Standard CSA-A23.3-94. Canadian Standards Association (CSA), Rexdale, Ont.

Demers, M., and Neale, K.W. 1994. Strengthening of concrete columns with unidirectional composite sheets. *In* Developments in Short and Medium Span Bridge Engineering '94, Proceedings of the 4th International Conference on Short and Medium Bridges, Halifax, N.S., 8–11 August 1994. *Edited by* A.A. Mufti, B. Bakht, and L.G. Jaeger. Canadian Society for Civil Engineering, Montréal, Que. pp. 895–905.

Demers, M., and Neale, K.W. 1999. Confinement of reinforced concrete columns with fibre-reinforced composite sheets—an experimental study. Canadian Journal of Civil Engineering, **26**: 226–241.

Harries, K.A., and Kharel, G. 2003. Experimental investigation of the behavior of variably confined concrete. Cement and Concrete Research, **33**: 873–880.

Howie, I., and Karbhari, V.M. 1995. Effect of tow sheet composite wrap architecture on strengthening of concrete due to confinement. I: Experimental studies. Journal of Reinforced Plastics & Composites, **14**: 1008–1030.

Jaffry, S.A.D., and Sheikh, S.A. 2001. Concrete-filled glass fibre-reinforced polymer (GFRP) shells under concentric compression. Department of Civil Engineering, University of Toronto, Toronto, Ont. Research Report SJ-01-01.

Karabinis, A.I., and Rousakis, T.C. 2002. Concrete confined by FRP material: a plasticity approach. Engineering Structures, **24**: 923–932.

Karbhari, V.M., and Gao, Y. 1997. Composite jacketed concrete under uniaxial compression—verification of simple design equations. ASCE Journal of Materials in Civil Engineering, **9**(4): 185–193.

Kestner, J.T., Harries, K.A., Pessiki, S.P., Sause, R., and Ricles, J.M. 1997. Rehabilitation of reinforced concrete columns using fiber reinforced polymer composite jackets. Center for Advanced Technology for Large Structural Systems, Lehigh University, Bethlehem, Pa. ATLSS Report No. 97-07.

Kshirsagar, S., Lopez-Anido, R.A., and Gupta, R.K. 2000. Environmental aging of fiber-reinforced polymer-wrapped concrete cylinders. ACI Materials Journal, **97**(6): 703–712.

Lin, C.-T., and Li, Y.-F. 2003. An effective peak stress formula for concrete confined with carbon fiber reinforced plastics. Canadian Journal of Civil Engineering, **30**: 882–889.

Lin, H., and Liao, C. 2004. Compression strength of reinforced concrete column confined by composite material. Composite Structures, **65**: 239–250.

Mandal, S., Hoskin, A., and Fam, A. 2005. Influence of concrete strength on confinement effectiveness of fiber-reinforced polymer circular jackets. ACI Structural Journal, **102**(3): 383–392.

Mastrapa, J.C. 1997. The effect of construction bond on confinement with FRP composites. M.Sc. thesis, University of Central Florida, Orlando, Fla.

Matthys, S., Taerwe, L., and Audenaert, K. 1999. Test on axially loaded concrete columns confined by fiber reinforced polymer sheet wrapping. *In* Proceedings of the 4th International Symposium on Fiber Reinforced Polymer Reinforcement for Concrete Structures (FRPRCS-4), Baltimore, Md., 31 October – 5 November 1999. *Edited by* C.W. Dolan, S.H. Rizkalla, and A. Nanni. ACI International, Farmington Hills, Mich. SP-188, pp. 217–229.

Mirmiran, A., Shahawy, M., Samaan, M., Echary, H.E., Mastrapa, J.C., and Pico, O. 1998. Effect of column parameters on FRP-confined concrete. ASCE Journal of Composites for Construction, **2**(4): 175–185.

Miyauchi, K., Nishibayashi, S., and Inoue, S. 1997. Estimation of strengthening effects with carbon fiber sheet for concrete columns. *In* Proceedings of the 3rd International Symposium on Non-metallic (FRP) Reinforcement for Concrete Structures, Sapporo, Japan, 14–16 October 1997. Japan Concrete Institute, Tokyo, Japan. Vol. 1., pp. 217–224.

Nanni, A., and Bradford, N.M. 1995. FRP jacketed concrete under uniaxial compression. Construction and Building Materials, **9**(2): 115–124.

Punshi, V., and Sheikh, S.A. 2003. Non-linear analysis of circular FRP-confined concrete columns using finite element methods. Department of Civil Engineering, University of Toronto, Toronto, Ont. Research Report, PS-01-03.

Purba, B.K., and Mufti, A.A. 1999. Investigation of the behavior of circular concrete columns reinforced with carbon fiber reinforced polymer (CFRP) jackets. Canadian Journal of Civil Engineering, **26**: 590–596.

Richart, F.E., Brandtzaeg, A., and Brown, R.L.1928. A study of the failure of concrete under combined compressive stresses. University of Illinois, Urbana, Ill. Engineering Experimental Station Bulletin No. 185.

Richart, F.E., Brandtzaeg, A., and Brown, R.L. 1929. The failure of plain and spirally reinforced concrete in compression. University of Illinois, Urbana, Ill. Engineering Experimental Station Bulletin No. 190.

Saatcioglu, M., and Ozcebe, G. 1989. Response of reinforced concrete columns to simulated seismic loading. ACI Structural Journal, **86**(1): 3–12.

Saffi, M., Toutanji, H.A., and Li, Z. 1999. Behavior of concrete columns confined with fiber reinforced polymer tubes. ACI Materials Journal, **96**(4): 500–509.

Shahawy, M., Mirmiran, A., and Beitelman, T. 2000. Tests and modeling of carbon-wrapped concrete columns. Composites Part B: Engineering, **31**: 471–480.

Sheikh, S.A., and Uzumeri, S.M. 1980. Strength and ductility of tied concrete columns. ASCE Journal of the Structural Division, **106**(5): 1079–1102.

Sheikh, S.A., and Yeh, C.C. 1990. Tied concrete columns under axial load and flexure. ASCE Journal of Structural Engineering, **116**(10): 2780–2801.

Soudki, K.A., and Green, M.E. 1996. Performance of CFRP retrofitted concrete columns at low temperature. *In* Advanced Composite Materials in Bridges and Structures, Proceeding of the 2nd International Conference, Montréal, Quebec, 11–14 August 1996. *Edited by* M.M. El-Badry. Canadian Society for Civil Engineering, Montréal, Que. pp. 427–434.

Theriault, M., Neale, K.W., and Claude, S. 2004. Fiber-reinforced polymer-confined circular concrete columns: investigation of size and slenderness effects. ASCE Journal of Composites for Construction, **8**(4): 323–331.

Toutanji, H.A. 1999. Stress–strain characteristics of concrete columns externally confined with advanced fiber composite sheets. ACI Materials Journal, **96**(3): 397–404.

Toutanji, H., and Deng, Y. 2002. Strength and durability performance of concrete axially loaded members confined with SFRP composite sheets. Composites Part B: Engineering, **33**: 255–261.

Uomoto, T., and Nishimura, T. 1999. Deterioration of aramid, glass, and carbon fibers due to alkali, acid, and water in different temperatures. *In* Proceedings of the 4th International Symposium on Fiber Reinforced Polymer Reinforcement for Concrete Structures (FRPRCS-4), Baltimore, Md., 31 October – 5 November 1999. *Edited by* C.W. Dolan, S.H. Rizkalla, and A. Nanni. ACI International, Farmington Hills, Mich. SP-188, pp. 515–522.

Watanabe, K., Nakamura, H., Honda, T., Toyoshima, M., Iso, M., Fujimaki, T., Kaneto, M., and Shirai, N. 1997. Confinement effect of FRP sheet on strength and ductility of concrete cylinders under uniaxial compression. Proceedings of the 3rd International Symposium on Non-metallic (FRP) Reinforcement for Concrete Structures, Sapporo, Japan, 14–16 October 1997. Japan Concrete Institute, Tokyo, Japan. Vol. 1, pp. 233–240.

Xiao, Y., and Wu, H. 2000. Compressive behavior of concrete confined by carbon fiber composite jackets. ASCE Journal of Materials in Civil Engineering, **12**(2): 139–146.

Zhang, S., Ye, L., and Mai, Y.W. 2000. A study on polymer composite strengthening systems for concrete columns. Applied Composite Materials, **7**: 125–138.

## List of symbols

$a$ ratio of strain at initiation of fibre rupture to the rupture strain from tensile coupon test ($0 < a < 1$)
$A_{\mathrm{core\ conc}}$ core concrete area
$A_{\mathrm{gross\ conc}}$ total concrete area
$b$ fraction of intact fibres at initiation of fibre rupture
$e_i$ energy capacity corresponding to $i$% of $f_{\mathrm{ccmax}}$ on descending branch
$d$ diameter of fibre filament
$D$ diameter of column
$E_{\mathrm{t}}$ initial tangent modulus of concrete
$f_{\mathrm{c}}'$ unconfined concrete strength obtained from standard cylinder tests
$f_{\mathrm{cc}}$ axial stress in confined concrete
$f_{\mathrm{ccmax}}$ confined concrete strength
$f_{\mathrm{co}}'$ unconfined concrete strength obtained from control specimen
$F_{\mathrm{u}}$ load at which FRP will fail based on assumption of linear elastic property
$K_1$ strength enhancement with respect to column concrete strength
$K_2$ strength enhancement with respect to cylinder concrete strength
$L$ length of column
$P_{\mathrm{conc}}$ load carried by concrete
$P_{\mathrm{max}}$ load capacity of column
$P_{\mathrm{steel}}$ load carried by steel
$P_{\mathrm{total}}$ total load applied on column
$W_i$ work index corresponding to $i$% of $f_{\mathrm{ccmax}}$ at descending branch
$\varepsilon$ axial strain
$\varepsilon_{\mathrm{cc}}$ concrete axial strain corresponding to $f_{\mathrm{ccmax}}$
$\varepsilon_{\mathrm{co}}$ concrete axial strain corresponding to $f_{\mathrm{co}}'$
$\varepsilon_{\mathrm{rup}}$ rupture strain of GFRP tensile coupon
$\varepsilon_0$ axial strain corresponding to $f_{\mathrm{ccmax}}$ on the initial tangent $E_{\mathrm{t}}$
$\varepsilon_2$ axial strain corresponding to a strength of $0.8f_{\mathrm{ccmax}}$
$\varepsilon_{50\mathrm{u}}$ concrete axial strain corresponding to $0.50f_{\mathrm{co}}'$ on descending branch of stress–strain curve
$\mu$ ductility factor
$\rho_{\mathrm{l}}$ ratio of area of longitudinal steel to that of cross section
$\rho_{\mathrm{s}}$ volumetric ratio of lateral steel to concrete core